Journal of Materials Chemistry C

Accepted Manuscript

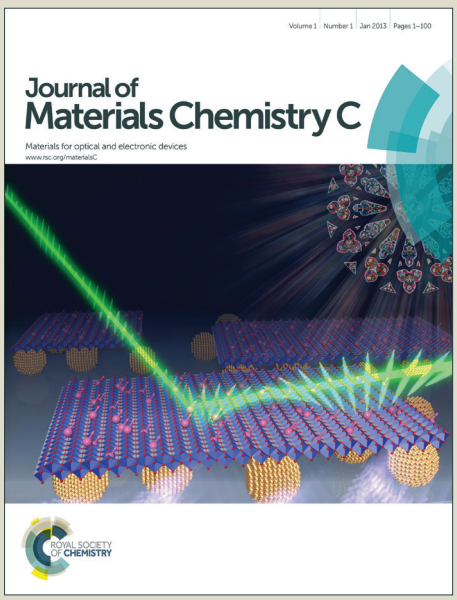

ROYAL SOCIETY OF CHEMISTRY

www.rsc.org/materialsC

Molecular weight sensing properties of ionic liquid-polymer composite films: theory and experiment†

Bishnu P. Regmi,[a] Nicholas C. Speller,[a] Michael J. Anderson,[b] Jean Olivier Brutus,[c] Yonathan Merid,[a] Susmita Das,[a] Bilal El-Zahab,[d] Daniel J. Hayes,[e] Kermit K. Murray,[a] and Isiah M. Warner*[a]

[a]Department of Chemistry, Louisiana State University, Baton Rouge, LA 70803, USA.
[b]Department of Chemistry, Columbus State University, Columbus, GA 31907, USA
[c]Biomedical Engineering Department, State University of New York at Stony Brook, Stony Brook, NY 11790, USA
[d]Mechanical and Materials Engineering Department, College of Engineering and Computing, Florida International University, Miami, FL 33174, USA
[e]Department of Biological and Agricultural Engineering, Louisiana State University, Baton Rouge, LA 70803, USA.
†Electronic supplementary information (ESI) available
*Corresponding author: Tel: +1225-578-2829. Fax: +1 225-578-3971. E-mail: iwarner@lsu.edu

Abstract

Ionic liquids (ILs) are rapidly emerging as important coating materials for highly sensitive chemical sensing devices. In this regard, we have previously demonstrated that a quartz crystal microbalance (QCM) coated with a binary mixture of an IL and cellulose acetate can be employed for detection and molecular weight estimation of organic vapors (*J. Mater. Chem*. 2012, **22**, 13732). Herein, we report follow-up studies aimed at formulating the theoretical basis for our previously observed relationship between molecular weight and changes in the QCM parameters. In the current work, we have investigated the vapor sensing characteristics of a series of binary blends of ILs and polymers over a wider concentration range of analytes, and a quadratic equation for estimating the approximate molecular weight of an organic vapor is proposed. Additionally, the frequency (*f*) and dissipation factor (*D*) at multiple harmonics were measured by use of a quartz crystal microbalance with dissipation monitoring (QCM-D). These QCM-D data were then analyzed by fitting to various models. It is observed that the behavior of these films can be best described by use of the Maxwell viscoelastic model. In light of these observations, a plausible explanation for the correlation between molecular weight of absorbed vapors and the QCM parameters is presented. Our previous findings appear to be a special case of this more general observation. Overall, these results underscore the true potential of IL-based composite materials for discrimination and molecular weight estimation of a broad range of chemical vapors.

KEYWORDS: QCM; dissipation; ionic liquids; GUMBOS; volatile organic compounds; molecular weight determination

Introduction

At present, there has been a rapid increase in interest in the development of high performance sensors for volatile organic compounds (VOCs) owing to the ever expanding need to monitor a wide array of chemical vapors in different environments. Specifically, VOC vapor sensors have proven to be very useful for 1) analysis of exhaled breath in evaluating medical conditions and environmental exposure to volatile toxins, 2) detection and discrimination of bacterial pathogens in medicine and industry, 3) examination of quality of food and beverages, and 4) assessment of environmental pollution.[1-6] In this regard, several research groups are involved in developing improved sensing devices for detection and discrimination of pure as well as complex mixtures of VOCs. The vast majority of these studies have employed the concept of sensor arrays.[7-17] In a sensor system, sensing materials are important components that play a key role in successful design and implementation of the sensor. Therefore, there is a recent upsurge of interest in the design and synthesis of improved sensing materials to couple with a variety of physical transducers. In this regard, the best combination of a sensing material and transducer is often sought to obtain optimal sensing performance.

Among a number of sensing technologies, sensors built on the use of acoustic wave-based transducers are favored for detection and discrimination of chemical vapors because such devices are often sensitive, compact, and amenable to creation of sensor arrays. In an acoustic wave sensor, a piezoelectric substrate is excited using an AC voltage to generate an acoustic wave that subsequently interacts with the surrounding medium, thereby probing its properties. Among different classes of acoustic wave devices, the thickness shear mode (TSM) resonator, better known as a quartz crystal microbalance (QCM), has been demonstrated to be a sensitive analytical tool for detection of chemical and biological species, as well as for probing interfacial properties and phenomena.

The use of a QCM device for chemical sensing entails immobilization of a thin film of sensing materials on the surface of the quartz crystal resonator (QCR), and the successful use of a QCM sensor relies on the performance of these materials. In this regard, ionic liquids (ILs) have emerged as promising sensing materials for QCM-based detection of a wide variety of organic vapors.[10,18-20] ILs are organic salts with melting points below 100 °C. ILs that are liquid at room temperature are commonly known as room temperature ionic liquids (RTILs), whereas those that are solid at room temperature are referred to as frozen ionic liquids. In our studies, we define frozen ionic liquids and related organic salts with melting points up to 250 °C collectively as a group of uniform materials based on organic salts (GUMBOS). High thermal stability, non-volatility, tunable physicochemical properties, chemical stability and ease of synthesis make ILs and GUMBOS ideal candidates for gas sensing applications. In addition, these

materials provide rapid and reversible response to various VOCs. More importantly, ILs and GUMBOS promote viscoelastic properties in composites which allow measurement of two QCM responses, thereby providing greater analytical information for vapor sensing studies.

We have recently reported results of vapor sensing using a QCM sensor prepared by depositing a thin film of a composite material comprising a binary mixture of GUMBOS and cellulose acetate (CA).[20] Interestingly, a very notable relationship between the ratio $\Delta f/\Delta R$ (where Δf refers to frequency change and ΔR refers to motional resistance change) and the molecular weight of the absorbed analytes was discovered. While this observation was very useful, the data were not sufficient to fully explain the unique vapor sensing characteristics of these films. It must be emphasized that a fundamental understanding of the material characteristics is essential to realizing the full potential of these materials.

In the present study, we have systematically investigated a number of IL-polymer combinations to fully evaluate the superior vapor sensing capabilities of this class of materials. A series of heterogeneous thin films comprising binary blends of an IL and polymer were immobilized on the QCR surface, and the reponse of the sensor toward a wide array of organic vapors over an extended concentration range was monitored. Solid phase (i.e. GUMBOS) as well as liquid phase ILs with a range of viscosities were investigated. Two different polymers—cellulose acetate (CA) and polymethylmethacrylate (PMMA)—were utilized to prepare these composite films. In addition, two types of interface electronics, one based on the use of an oscillator circuit and another based on a ring-down approach, were used to measure the QCM responses. Based on these new observations over an extended concentration range of analytes, a quadratic equation for estimation of the molecular weight of organic vapors is proposed. Additionally, the frequency (f) and dissipation (D) at multiple harmonics, as measured by use of a quartz crystal microbalance with dissipation monitoring (QCM-D), were fitted to different materials models. Excellent agreement between the experimental data and theoretical values predicted by use of the Maxwell viscoelastic model was observed. In light of these observations, we propose a theoretical model to explain our previous as well as current observations relating QCM parameters with the molecular weight of absorbed volatile analytes. Assessment of our overall data suggests that the observed molecular weight relationship for this class of materials has a sound theoretical basis. Overall, these materials exhibit truly unique sensing characteristics which make the QCM sensor an even more promising tool with capabilities for detection, discrimination, and molecular weight determination of a wide range of chemical vapors.

Theory of QCM

The QCR comprises a thin plate of AT-cut quartz crystal coated on each face with thin metallic electrodes. Owing to the piezoelectric properties of quartz, application of an AC voltage across the quartz crystal causes oscillations in the thickness shear mode with resonance frequencies in the megahertz (MHz) range. This shear wave experiences a frequency shift and attenuation as it is transmitted through the sensing film immobilized on the electrode surface. The mass and mechanical properties of the coating, which determine the acoustic load at the interface, are perturbed as an analyte interacts with the coating material resulting in alteration of the propagation characteristics (phase and amplitude) of the shear waves. The resonance behavior of the QCM is described by two essential parameters, and in this regard three different types of interface electronics have been commonly employed to measure these quantities. A simple way to accomplish QCM measurements is by use of an oscillator circuit which gives frequency shift (Δf) and motional resistance shift (ΔR) as output parameters.[21,22] However, oscillator circuits are limited to only one harmonic, which makes it difficult to interpret the acquired data. Another kind of interface electronics used to acquire QCM parameters employs an impedance analyzer, and this provides frequency shift (Δf) and bandwidth shift ($\Delta \Gamma$) at different harmonics.[22-24] A relatively new approach to QCM measurements introduced by Kasemo and coworkers,[25,26] is a ring-down-based technique, and this allows measurement of frequency shift (Δf) and dissipation factor shift (ΔD) over a range of odd harmonics. In fact, the QCM-D instrumentation is based on this ring-down approach.

Motional resistance (R), bandwidth (Γ), and dissipation factor (D) are equivalent parameters; all of them represent energy loss during oscillation, and are therefore related as follows:[25-27]

$$D = \frac{E_{dissipated}}{2\pi E_{stored}} \quad (1), \qquad D = \frac{2\Gamma}{f} \quad (2), \text{ and} \qquad D = \frac{R}{2\pi f L} \quad (3)$$

where f is the resonance frequency, L is the motional inductance of the Butterworth-van Dyke equivalent circuit of QCR, $E_{dissipated}$ is the energy lost per oscillation cycle, and E_{stored} is the total energy stored in the system.

It is well documented that the resonance frequency of a QCR system decreases when the surface of the crystal is loaded with a mass. For a thin and rigid film uniformly coated on the surface, the relationship between resonance frequency shift (Δf) and the mass adsorbed can be expressed by the well-known Sauerbrey equation as follows:[28]

$$\Delta f = -\frac{n}{C}\Delta m = -\frac{n}{C}\rho_f t_f \qquad (4)$$

where Δm is mass per unit area of the film, ρ_f is the density of the film, t_f is the thickness of the film, n is the harmonic number which can only be an odd integer, and C is the mass sensitivity or Sauerbrey constant which depends on the fundamental resonance frequency and properties of the quartz (C = 17.7 ng.cm^{-2}.Hz^{-1} for a 5 MHz AT-cut quartz crystal). If the film is thin and rigid, it has the properties of an ideal mass layer and the change in dissipation factor is zero. However, the films used in many QCM-based applications are viscoelastic, and hence dissipate energy during oscillations. For such films, the frequency change is a function of both mass and viscoelastic properties of the coating material. The rheological behavior of viscoelastic materials can be characterized by a complex shear modulus (G^*), and thus $G^* = G' + iG''$, where G' (or μ) is the elastic shear modulus and G'' is the loss modulus. Several mathematical models have been proposed for simulation of the viscoelastic properties of materials. Two commonly used models in this regard are the Maxwell model, in which a spring and dashpot are connected in series, and the Kelvin-Voigt model, in which the spring and dashpot are arranged in parallel.

The frequency and dissipation changes of a QCR coated with a thin layer of Maxwell viscoelastic material, which is consistent with the present study, is given as follows:[29]

$$\Delta f \approx -\frac{t_f \rho_f \omega}{2\pi\rho_q t_q}\left(1 + \frac{t_f^2 \rho_f \omega^2}{3\mu}\right) \qquad (5), \quad \text{and}$$

$$\Delta D \approx \frac{2 t_f^3 \rho_f^2 \omega}{3\rho_q t_q \eta} \qquad (6),$$

where ρ_q is the density of the quartz, t_q is the thickness of the quartz, ω is the angular frequency, μ is the elastic shear modulus of the film, and η is the viscosity of the film. The first term in equation 5 is in fact the Sauerbrey mass, while the second term represents the viscoelastic correction to the Sauerbrey mass. It is evident from equations 5 and 6 that the mass correction depends on the elasticity of the film, while the dissipation depends only on the viscosity of the film. Similar equations have been derived for Kelvin-Voigt materials where the mass correction, as well as dissipation factor, is found to depend on both the elasticity and viscosity of the film.[29,30] Despite the fact that these two parameters can be simultaneously obtained in QCM measurements, the vast majority of previous studies have focused only on measuring Δf as a function of analyte concentration. However, it is clear that monitoring both parameters in QCM studies is much more informative for many applications. It should be noted that not all sensing materials provide this two-parameter response, and hence the selection of suitable sensing materials is important.

Experimental section

Materials

Four ILs 1-butyl-2,3-dimethylimidazolium hexafluorophosphate ([BM_2Im][PF_6]), 1-hexyl-3-methylimidazolium hexafluorophosphate ([HMIm][PF_6]), 1-hexyl-3-methylpyridinium hexafluorophosphate ([HMPyr][PF_6]), and 1-hexyl-3-methylpyridinium bis(trifluoromethane)sulfonimide ([HMPyr][TFSI]); and two polymers cellulose acetate (CA) and poly(methyl methacrylate) (PMMA) were used to prepare coatings for the present studies. The compound [BM_2Im][PF_6] was obtained from Ionic Liquids Technologies, Inc. (Tuscaloosa, AL, USA) as a crystalline solid and [HMIm][PF_6] was obtained from TCI America, Inc. (Portland, OR, USA) as a liquid. PMMA (molecular weight ~500,000 Da) was obtained from Polysciences, Inc. (Warrington, PA, USA). CA (average molecular weight ~30,000 Da), anhydrous heptane, anhydrous acetonitrile, anhydrous chloroform, anhydrous toluene, anhydrous methanol, anhydrous ethyl acetate, anhydrous 1-propanol, anhydrous 2-propanol, anhydrous 1-butanol, p-xylene, 3-picoline, 1-bromohexane, lithium *N*,*N*-bis-(trifluoromethane)sulfonimide (LiTFSI), potassium hexafluorophosphate (KPF_6) were obtained from Sigma-Aldrich (St. Louis, MO, USA). Acetone and dichloromethane were obtained from Avantor Performance Materials, Inc. (Center Valley, PA, USA). Absolute ethanol was obtained from Pharmco Products, Inc. (Brookfield, CT, USA). All chemicals were used as received without further purification.

Two different QCM instruments, one based on an oscillator circuit (QCM200) and the other based on an impulse excitation technique (QCM-D), were used in the studies presented here. Crystals with a fundamental resonance frequency of 5 MHz were used in both instruments. The QCM200 system and optically polished chromium/gold AT-cut quartz crystals with a diameter of 1" were purchased from Stanford Research Systems, Inc. (Sunnyvale, CA, USA). The QCM-D E4 system and optically polished gold-coated AT-cut quartz crystals with a diameter of 14 mm were obtained from Q-Sense AB (Gothenburg, Sweden). Mass flow controllers (Model 5850E) and instrument control and read out equipment (Model 5878) were obtained from Brooks Instrument, LLC (Hatfield, PA, USA). The polytetrafluoroethylene (PTFE) containers were purchased from SPI Supplies/ Structure Probe, Inc. (West Chester, PA, USA).

Synthesis of ionic liquids

The compounds [HMPyr][PF_6] and [HMPyr][TFSI] were synthesized using a two-step procedure.[31] Briefly, equimolar amounts of 3-picoline and 1-bromohexane were refluxed at 65 °C for 40 hours. The resulting product was washed several times with ethyl acetate and finally rotovaped to obtain a viscous light yellow liquid [HMPyr][Br]. Then, [HMPyr][Br] was dissolved in water and a slight excess of aqueous KPF_6 was added and stirred overnight at room temperature to obtain [HMPyr][PF_6]. The product was washed several times with water and freeze-dried to remove water in order to obtain a highly viscous light yellow liquid. [HMPyr][TFSI] was prepared similarly by reacting [HMPyr][Br] with LiTFSI. The product was found to be a colorless liquid of low viscosity.

Preparation of stock solutions

Stock solutions of 1 mg/mL ionic liquids were prepared in acetone. A stock solution of 0.5 mg/mL cellulose acetate was prepared in acetone, and a stock solution of 1 mg/mL PMMA was prepared in dichloromethane.

Cleaning of quartz crystals

The quartz crystal was rinsed with distilled water followed by acetone and finally with dichloromethane. The crystal was carefully dried using flowing nitrogen, and then immersed in fresh piranha solution (3:1 concentrated sulfuric acid and 30% hydrogen peroxide) until no bubbles were seen (usually 5-10 minutes), followed by rinsing with copious amounts of distilled water. The crystal was further rinsed with acetone and then dichloromethane followed by drying under a stream of nitrogen. The crystal was placed in an oven at 100 °C until it was completely dry, and subsequently allowed to cool to room temperature before film deposition.

Thin film preparation and characterization

Thin films were deposited on the surface of the QCR using a solvent precipitation method that has been previously described.[20] Freshly prepared stock solutions were used for all coatings. To prepare an IL-only coating, a 600 µL stock solution of IL was diluted with acetone to a final volume of 2 mL, followed by addition of 6 mL of anhydrous heptane to the solution while stirring. The entire solution was placed in a 25 mL PTFE beaker, and a freshly cleaned crystal was dipped into the solution (the Q-Sense sensor crystal is smaller in diameter, and hence it was placed on top of the SRS quartz crystal) and left undisturbed for 6 hours. All ILs used in this study are soluble in acetone but insoluble in heptane. Acetone is more volatile and evaporates more rapidly, ultimately depositing a thin film on the substrate. To prepare IL-CA films, 160-200 µL of CA solution was added to 600 µL of IL solution and the mixture diluted with acetone to a final volume of 2 mL, while the subsequent steps were the same as defined

above. For preparation of the IL-PMMA film, 80-100 µL of PMMA solution (in dichloromethane) was added to 600 µL of IL solution and the mixture diluted with acetone to a final volume of 2 mL, and all subsequent steps were as defined above. Both cellulose acetate and PMMA are insoluble in heptane, and hence each is co-deposited with the IL. After incubation, residual heptane was drained and the crystal was ultrasonicated in a vertical position within a fresh pool of heptane for approximately 1 minute. The lower surface of the crystal was wiped using solvent-soaked cotton, and left to dry in a desiccator for at least 24 hours. The films were imaged using atomic force microscopy (AFM+, Anasys Instruments, Santa Barbara, CA) in tapping mode. An area of 80x80 μm^2 was scanned with 0.5 Hz scan rate using N-type tapping mode tips (AppNano, Mountain View, CA, ACCESS-NC, resonant frequency: *ca* 250 kHz) with a tip radius of 6 nm and nominal spring constant of 78 $N.m^{-1}$.

Vapor sensing studies

Two types of vapor delivery systems, static and dynamic, were used during vapor sensing studies. For measurements using the QCM200, a static system was used, while a flow system was used for QCM-D measurements. The experimental arrangement for the static system is reported in our previous publication.[20] All experiments were performed at 22 °C. A schematic diagram of the experimental setup with the flow-type system is shown in Fig. S1, ESI†. Again, all experiments were conducted at 22 °C. Each analyte vapor was generated by bubbling ultrapure argon through the liquid sample in a sealed container and the vapor was diluted with an additional stream of argon. The diluted vapor was then allowed to flow through a 1-meter-long tube to ensure complete mixing before reaching the sensor chamber. The flow rates of each of the two streams of argon were changed using two mass flow controllers (MFC1 and MFC2), while the total flow rate was adjusted to 100 sccm. The QCM-D E4 system was fitted with a flow module, and data acquired using the QSoft401 software.

Results and discussion

Chemosensitive film preparation and characterization

All sensing films used in these studies were prepared using the solvent precipitation method as previously described.[20] These films were characterized by optical microscopy (OM), scanning electron microscopy (SEM), and atomic force microscopy (AFM). Representative AFM images of two of the several films are shown in Fig. 1a-d. Fig. 1a is the AFM topographic image of approximately 90 $\mu g.cm^{-2}$ of $[BM_2Im][PF_6]$-PMMA, and Fig. 1b is the height profile following the blue line indicated in Fig. 1a. Similarly, Fig. 1c is the AFM topographic image of approximately the same amount of $[BM_2Im][PF_6]$-CA, and Fig. 1d is the height profile corresponding to the blue line indicated in Fig. 1c. From these images, it is evident that the

coatings comprise isolated microdroplets of varying size with heights reaching 2.7 μm. Coating-to-coating mass variations were found to be less than 10 percent. The heights measured by AFM and the heights measured by laser scanning confocal microscopy, as reported in our earlier publication,[20] are in very good agreement. All other films were characterized using OM and SEM, and all had similar isolated microdropets of varying dimensions (data not shown).

Vapor sensing studies using QCM

All QCM sensors were exposed to a variety of organic vapors as pure analytes, and changes in frequency and motional resistance were monitored simultaneously. Plots of the magnitude of Δf versus the concentration of VOC for a QCM sensor coated with [HMPyr][PF_6] are shown in Fig. S2a, ESI†. For each analyte, the best fit for the data is a second-degree polynomial with a downward curvature.

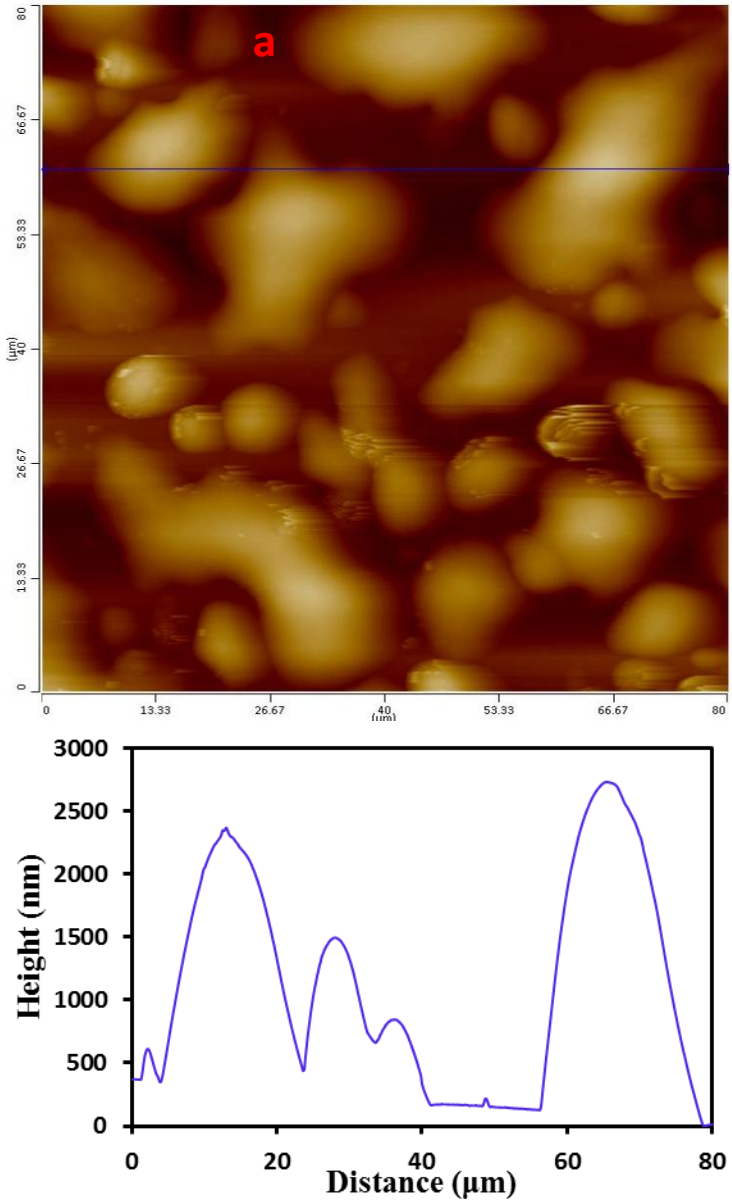

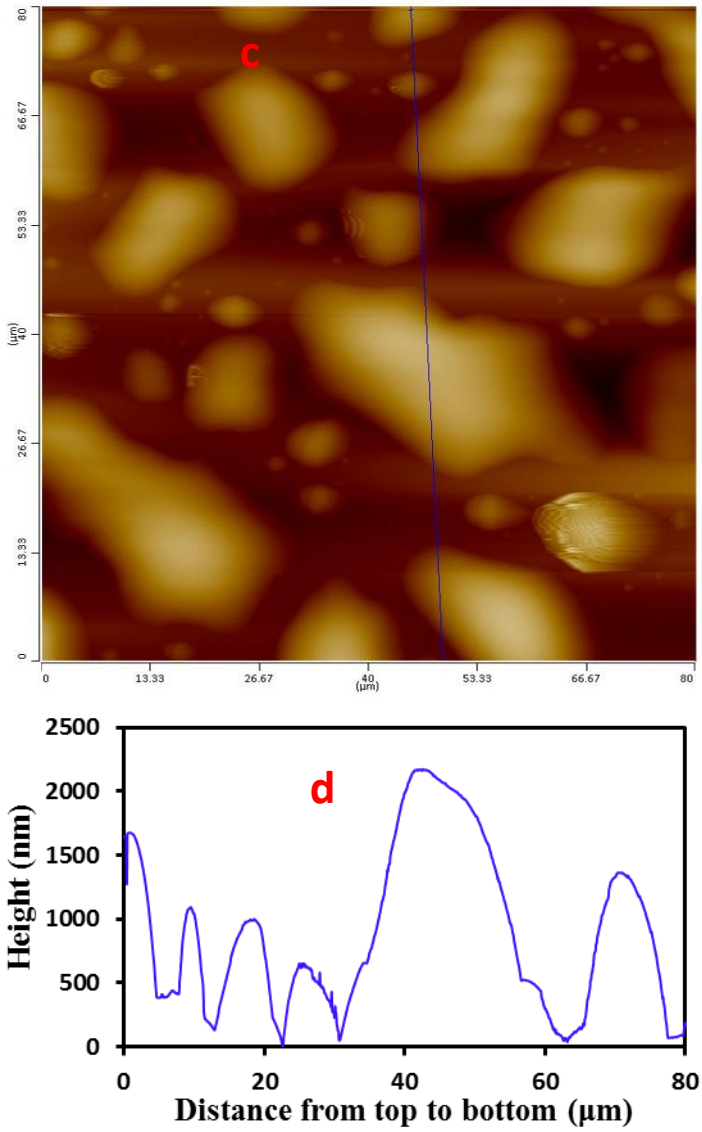

Fig. 1 (a) AFM topographic image of $[BM_2IM][PF_6]$-PMMA film. (b) Height profile corresponding to the horizontal blue line drawn in topographic image a. (c) AFM topographic image of $[BM_2IM][PF_6]$-CA film. (d) Height profile corresponding to the vertical blue line drawn in the image c. Amount of film material in each case is approximately 90 µg.cm^{-2}.

Similarly, a plot of ΔR against concentration of analytes is also a polynomial curve, but with upward curvature (Fig. S2b, ESI†). The plots of Δf versus ΔR for different analytes (only six analytes are shown for clarity) are displayed in Fig. 2. It is evident that each analyte shows a unique polynomial relationship between Δf and ΔR with a coefficient of determination (R^2) of unity or very close to unity. Therefore, simultaneous measurements of Δf and ΔR for a single QCM sensor enable an excellent discrimination of

chemical vapors irrespective of their concentration. On the other hand, a conventional QCM sensor, which is based on measurement of Δf alone, requires multiple sensors in order to achieve the same level of discrimination. In fact, a sensor based on two-parameter response, as demonstrated here, provides more information in array-based vapor sensing, thereby greatly enhancing vapor discrimination.

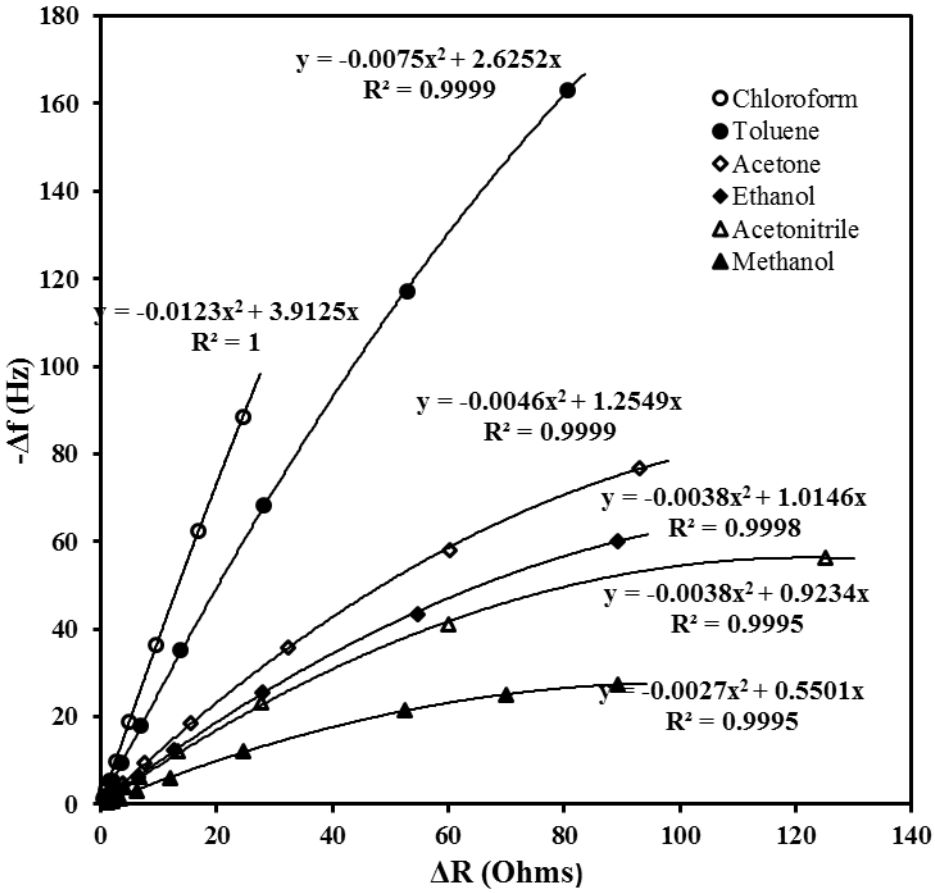

Fig. 2 Frequency shift versus motional resistance shift during vapor absorption by a QCM sensor coated with [HMPyr][PF_6].

An obvious question arises regarding a comparison of the above data involving pure ILs to binary mixtures similar to those obtained in our previous study. Thus, we evaluated the vapor sensing characteristics of a QCM coated with binary blends of [HMPyr][PF_6] and polymers. Two polymers including CA and PMMA were used for this study. Some notable differences in the sensing performance of the composite films as compared to that of the pure ionic liquid films were observed. Specifically, the slope of Δf versus concentration for composite films is found to increase for each analyte as compared to that of pure IL films, and these plots are primarily linear (Fig. S4 and S6, ESI†). In contrast, the slope of

the ΔR versus concentration plot for each composite film decreases as compared to that of the pure ionic liquid film (Fig. S5 and S7, ESI†). The relative values of the slopes of the Δf versus concentration plots for different analytes are quite different for pure IL films as compared to those of composite films (Fig. S2, S4, and S6, ESI†). However, the relative values of the slopes for the two composite films are essentially the same (Fig. S4 and S6, ESI†). It is noted that the relative slopes of ΔR versus concentration plots remain similar for all three films (Fig. S3, S5, and S7, ESI†). In short, all these observations imply that the ionic liquid is largely responsible for vapor absorption, whereas PMMA or CA modulates the viscoelastic properties of the ionic liquid.

A plot of Δf versus ΔR for the composite films, similar to the pure IL film, follows a second-degree polynomial for each analyte (Fig. 3). More importantly, when the Δf-ΔR plots for each vapor are divided by the molecular weight (MW) of the respective vapor, all curves merge into a single second-degree polynomial curve, and this is true only for the composite-coated QCM sensors. Fig. 4 is such a Δf/MW versus ΔR plot for a [HMPyr][PF_6]-PMMA coating exposed to nine different analytes—methanol, acetonitrile, ethanol, acetone, 2-propanol, nitromethane, dichloromethane, toluene, and chloroform—over an extended range of vapor concentrations. This plot has a R^2 of 0.998, which is a very remarkable correlation. Similar results were obtained for the [HMPyr][PF_6]-CA coated sensor (Fig.S8, ESI†). It is important to note that IL-PMMA film displayed better correlation as compared to IL-CA film. This could possibly be due to better mechanical stability of the IL-PMMA films; additional studies are needed to fully understand this observation.

To illustrate further, we investigated the vapor sensing characteristics of composite films prepared using other ionic liquids. The response of a [HMIm][PF_6]-PMMA coated sensor to 11 different analyte vapors (p-xylene and ethyl acetate in addition to the above-mentioned analytes) is shown in Fig. 5; and the response of the [BM_2Im][PF_6]-PMMA coated sensor to six different analytes is shown in Fig. 6. It is clear that the composite films prepared from all three ILs show similar behavior. The relationship between QCM parameters and molecular weight is not evident in the pure IL films (Fig. S9, ESI†). Hence, simultaneous measurements of Δf and ΔR for IL-polymer composite-coated QCM sensors during vapor exposure can be used to determine the approximate molecular weight of an unknown vapor with the following equation:

$$\mathrm{MW} = \frac{-\Delta f}{k'\Delta R^2 + k\Delta R} \qquad (7)$$

In this equation, k' and k are constants that are coating dependent. For instance, for the data from the [HMPyr][PF_6]-PMMA coating displayed in Fig. 4, k' is -0.00104 and k is 0.113. For all coatings in our

study, k' is much smaller than k. Hence, under low vapor absorptions (low values of ΔR), Equation 7 reduces to

$$\frac{\Delta f}{\Delta R} = -\mathrm{kMW} \quad (8),$$

which is consistent with the observations reported in our previous report. [20] In our earlier studies,

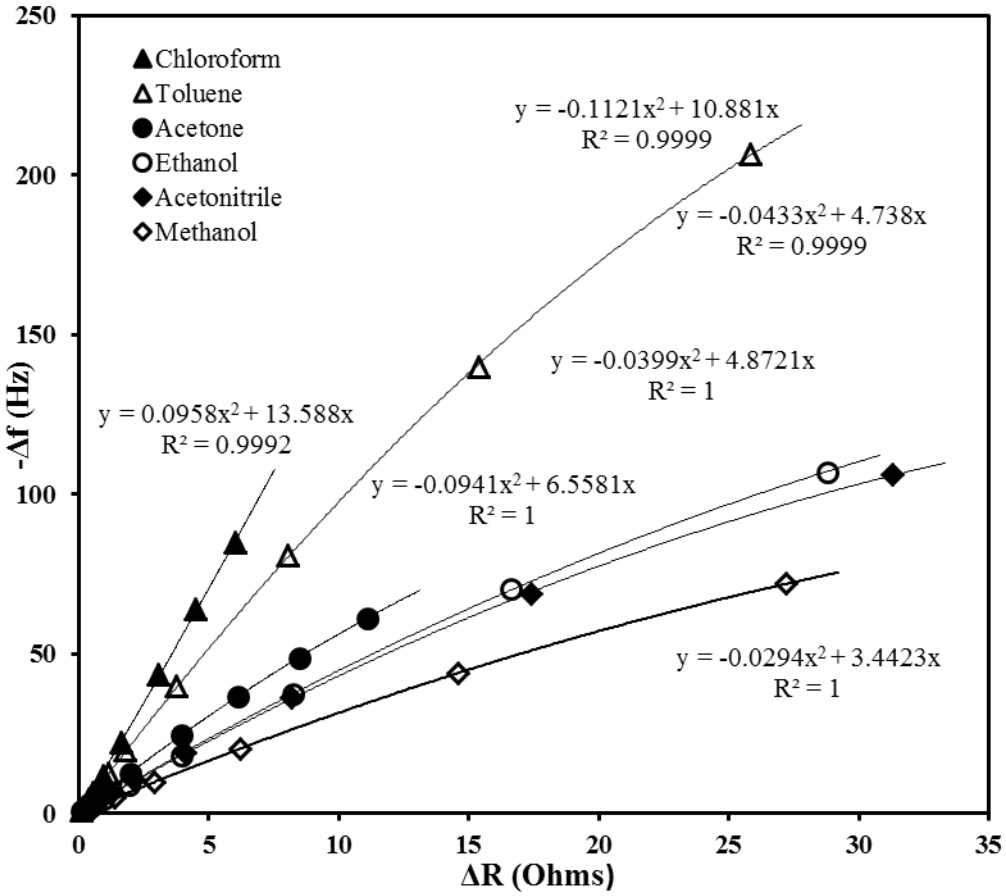

Fig. 3 Frequency shift versus motional resistance shift due to vapor absorption by a QCM sensor coated with [HMPyr][PF_6]-PMMA.

[BM_2Im][PF_6]-CA composite was used as the coating material. It is important to note that [BM_2Im][PF_6] is in the solid state at room temperature, and thus our previous studies were limited to solid phase ILs only. The present study confirms that highly viscous liquid phase ILs also show sensing characteristics similar to the solid phase ILs.

The sensor displayed a frequency noise of ~0.2 Hz, motional resistance noise of ~10 mΩ, and minimal drifts of both these parameters. The repeatability of the sensor response was evaluated by repeatedly exposing the sensors to various concentrations of acetonitrile and then evaluating the $\frac{\Delta f}{\Delta R}$ ratio. These sensors showed excellent repeatability with relative standard deviations (RSDs) for three replicate measurements between 1 and 4% (see Fig.S10, ESI†).

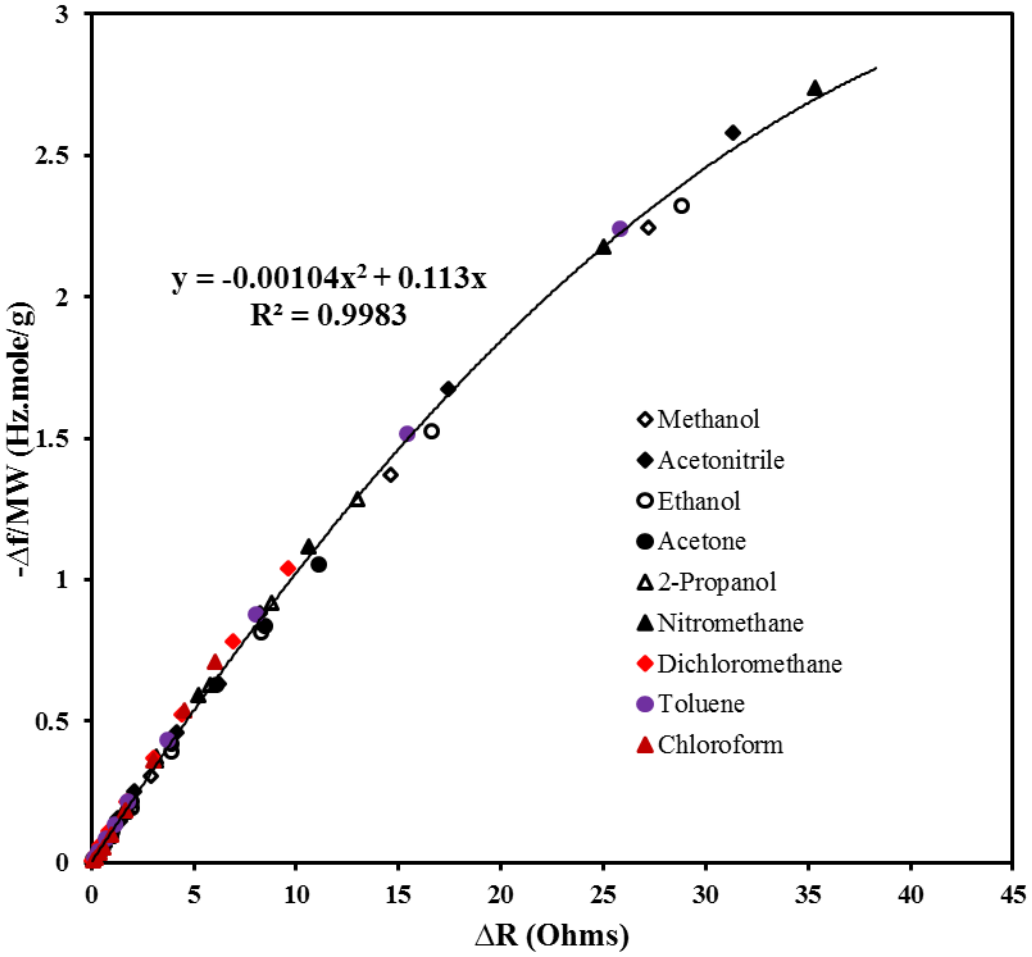

Fig. 4 Plot of the ratio of frequency shift to molecular weight against motional resistance shift of a QCM sensor coated with [HMPyr][PF_6]-PMMA for nine different organic vapors. Concentration ranges of the vapors are 0.574 to 45.9 mg L^{-1} for methanol, 0.114 to 11.4 mg L^{-1} for acetonitrile 0.382 to 38.2 mg L^{-1} for ethanol, 0.191 to 19.1 mg L^{-1} for acetone, 0.190 to 26.6 mg L^{-1} for 2-propanol, 0.138 to 6.88 mg L^{-1} for nitromethane, 0.321 to 64.2 mg L^{-1} for dichloromethane, 0.125 to 20.9 mg L^{-1} for toluene, and 0.216 to 29.0 mg L^{-1} for chloroform.

As pointed out above, an important parameter that greatly influences the sensor responses is the viscosity of the IL. Therefore, we decided to study the effects of changing the viscosity of the IL on the sensing performance of the sensor. It has been shown that TFSI anion-based ILs are much less viscous than PF_6 anion-based ILs.[32,33] Hence, [HMPyr][TFSI] was selected as a representative low viscosity IL for our studies. A film of [HMPyr][TFSI] exhibited slightly lower Δf (almost 20 percent lower), but much higher ΔR (more than five times) as compared to similarly prepared [HMPyr][PF_6] film. The [HMPyr][TFSI]-coated sensor upon exposure to different organic vapors produced a positive Δf as well as a positive ΔR. A plot of Δf versus ΔR was found to be linear with slopes dependent on the vapors (Fig. S11, ESI†); however, a correlation with the molecular weight was not apparent. In addition, binary blends of this IL with polymers did not improve the relationship of QCM parameters with molecular weight. Based on these observations, we conclude that ILs with higher viscosities (or solid phase equivalents, i.e. GUMBOS) are essential materials for achieving a direct correlation between molecular weight of measured analytes and changes in QCM parameters.

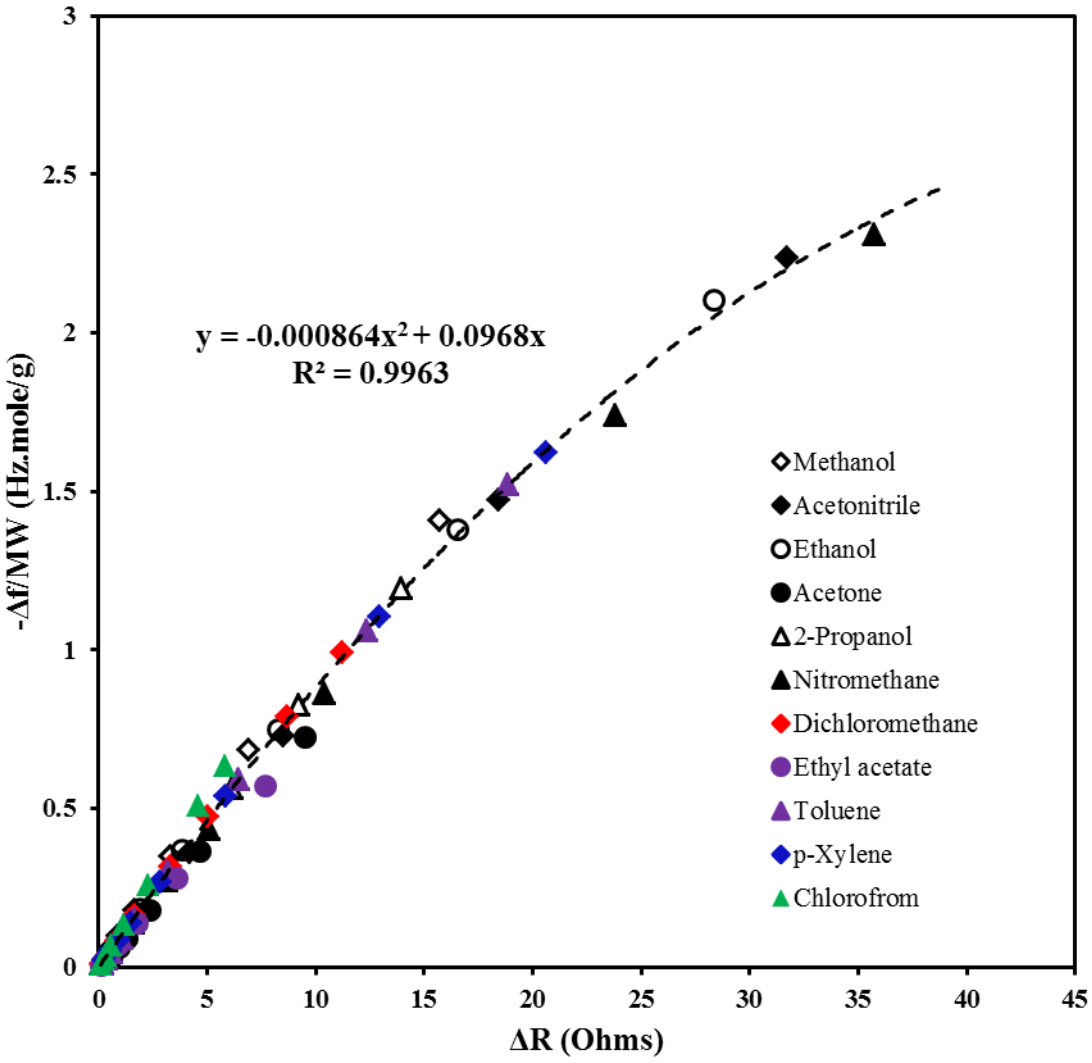

Fig.5 Plot of the ratio of frequency shift to molecular weight against motional resistance shift of a QCM sensor coated with [HMIm][PF_6]-PMMA for 11 different organic vapors. Concentration ranges of the vapors are 0.574 to 30.6 mg.L^{-1} for methanol, 0.114 to 11.4 mg.L^{-1} for acetonitrile 0.382 to 38.2 mg.L^{-1} for ethanol, 0.229 to 15.3 mg.L^{-1} for acetone, 0.190 to 26.6 mg.L^{-1} for 2-propanol, 0.138 to 6.88 mg.L^{-1} for nitromethane, 0.643 to 80.3 mg.L^{-1} for dichloromethane, 0.218 to 17.4 mg.L^{-1} for ethyl acetate, 0.125 to 20.9 mg.L^{-1} for toluene, 0.125 to 12.5 mg.L^{-1} for p-xylene, and 0.360 to 36.0 mg.L^{-1} for chloroform.

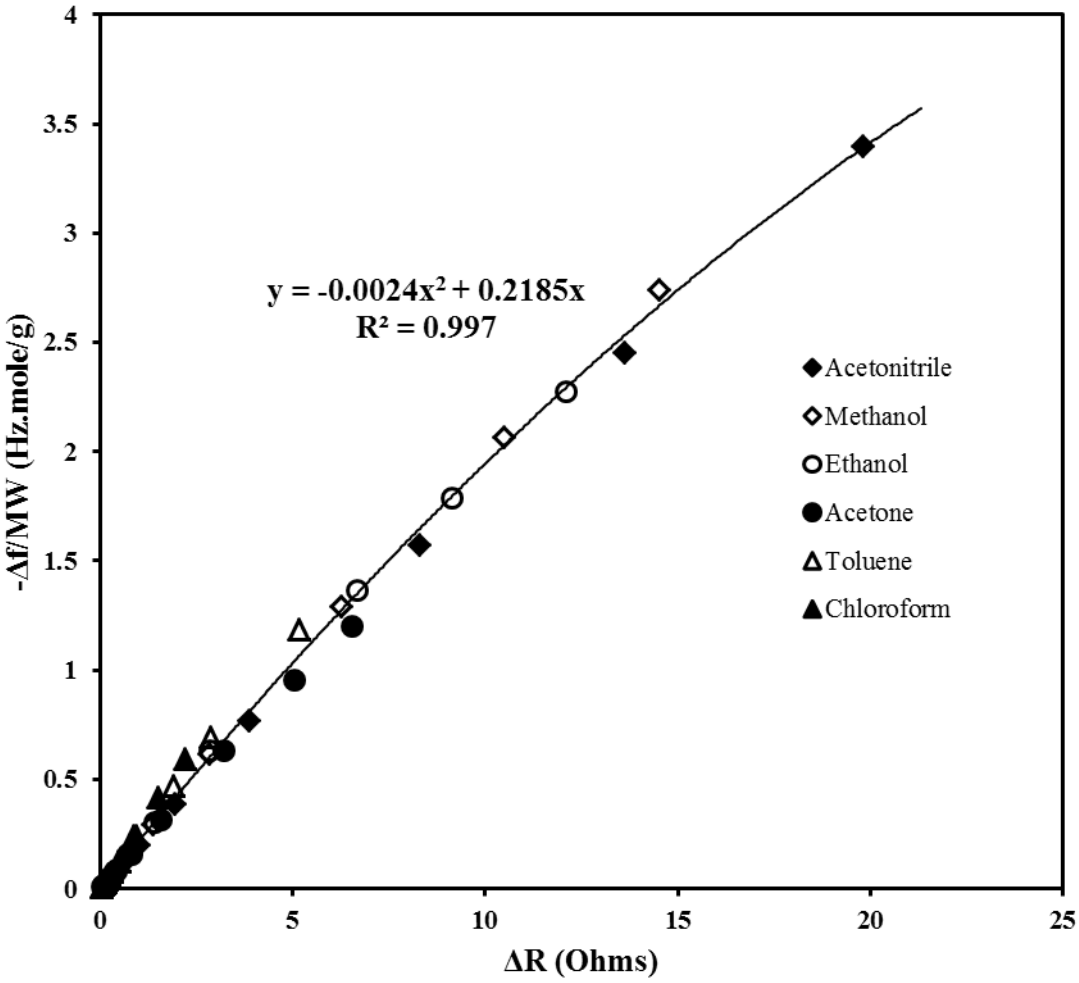

Fig. 6 Plot of the ratio of frequency shift to molecular weight against motional resistance shift of a QCM sensor coated with $[BM_2Im][PF_6]$-PMMA for six different organic vapors. Concentration ranges of the vapors are 0.574 to 57.4 $mg.L^{-1}$ for methanol, 0.114 to 15.2 $mg.L^{-1}$ for acetonitrile 0.382 to 45.8 $mg.L^{-1}$ for ethanol, 0.267 to 28.6 $mg.L^{-1}$ for acetone, 0.125 to 20.9 $mg.L^{-1}$ for toluene, and 0.360 to 36.0 $mg.L^{-1}$ for chloroform.

QCM-D studies and the theoretical basis for molecular weight estimation

In order to further elucidate the unique sensing behavior of these types of materials, additional studies were conducted using a QCM-D. For these QCM-D studies, a flow-type system was used to generate the analyte vapors where a stream of ultra-pure argon was bubbled through a liquid sample, and the vapors generated were subsequently diluted with another stream of argon to produce vapor of a desired concentration. Assuming the primary gas stream contains the saturated vapor of the analyte, the minimum concentration obtained was 1.0% of the saturation vapor pressure. Plots of Δf versus ΔD for the first harmonic of a $[HMPyr][PF_6]$-PMMA coated QCM-D sensor after exposure to eight different vapors are

shown in Fig. 7a. Similar to the Δ*f* versus Δ*R* plots, all Δ*f*-Δ*D* plots are second-degree polynomials, and each exhibits an R^2 close to unity. A plot of Δ*f*-to-MW ratio versus Δ*D* is shown in Fig. 7b. The relationship for molecular weight with Δ*f* and Δ*D* is observed to be very remarkable. Some analytes have slight deviations at high vapor concentrations. It is noted that the correlation of molecular weight with QCM-D parameters is even better with compounds belonging to the same class. For instance, the response for the five alcohols is shown in Fig. 8a. As expected, 1-propanol and 2-propanol were found to be indistinguishable (Fig. 8b). Plots of Δ*f* versus Δ*D* for the third and fifth harmonics were also found to be second-degree polynomials (see Fig. S12 and S13, ESI†). However, much larger deviations from the molecular weight relationship were observed. The frequency noise for the first harmonic was less than 0.1 Hz and dissipation noise was less than 0.02×10^{-6}. The response time was less than 20 seconds, while the recovery time was approximately 5 seconds. The repeatability of the sensor was assessed by repeating the measurements three times for methanol and ethanol vapors (see Fig. S14, ESI†). The RSD for both analytes was between 0.1 to 1%. The much higher repeatability of the QCM-D is attributed to better temperature control. We believe that a similar RSD is achievable for other analytes. Such high precision measurements are particularly important in differentiation of closely related analytes or mixtures.

Our QCM-D data were modeled using QTools software 3.0.17.560 provided by the manufacturer (Q-Sense AB). The Δ*f* and Δ*D* values of the first, third, and fifth harmonics (higher harmonics were not obtained) were used to model the data both before and during vapor uptake by the sensing films. The modeling of QCM-D data, acquired at different harmonics, to extract mass and other parameters of the film has been described in detail by several authors,[34-36] and similar procedures were applied to modeling our data. The film was treated as a single layer, and the density of the film was assumed to be 1300 $kg.m^{-3}$ and also assumed to remain unchanged during vapor absorption.[37] These data were fit to different mathematical models, and the goodness of fit for each model was judged by comparison of the chi-square (χ^2) value, which is defined as $\chi^2 = \sum_{i=1}^{l} [\{y_i(theory) - y_i(experiment)\}/\sigma_i]^2$, where y_i (theory) and y_i(experiment) represent modeled and measured values of Δ*f* or Δ*D*, respectively, and σ_i represents the associated noise. A smaller χ^2 indicates a better fit to the data set.[35,36] As a first assumption, the film was treated as if it were purely elastic, and hence η was set to zero, while the thickness (t_f) and elasticity (μ) were fit by the model.[34,35] The experimental Δ*f* and Δ*D* values were not consistent with the fit values (see Fig. S15, ESI†). The film was then assumed to be purely viscous by setting μ to zero, and fitting t_f and η to the model. The experimental Δ*f* and Δ*D* values were again not consistent with the fit values, (see Fig. S16, ESI†) suggesting that a purely viscous model cannot accurately describe the film.

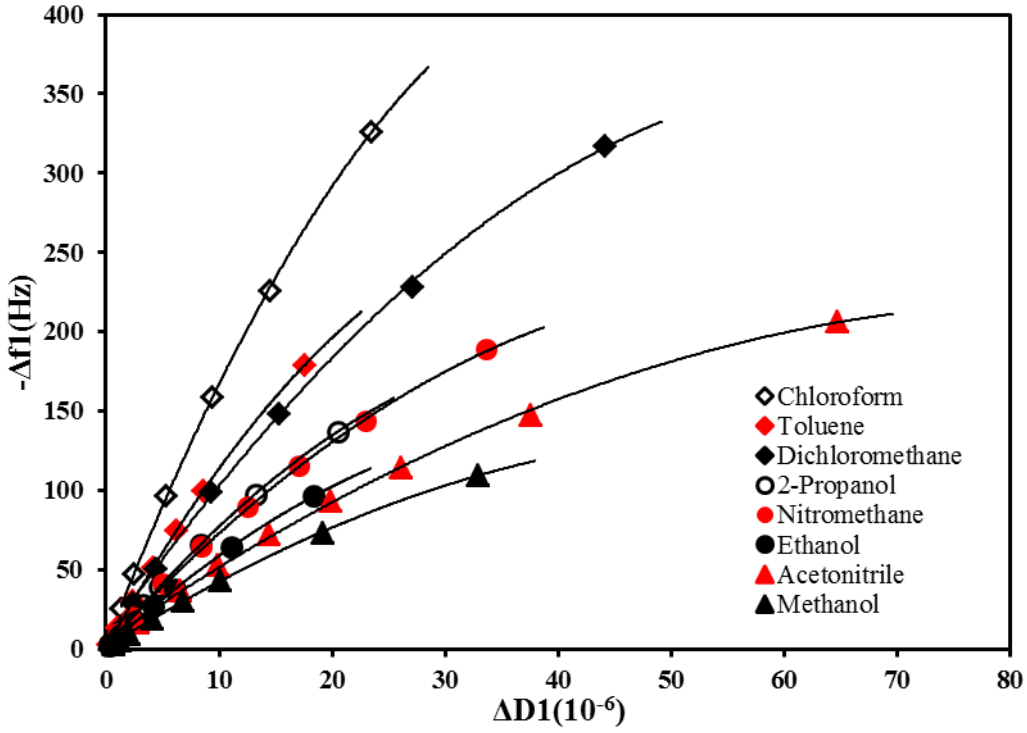

(a)

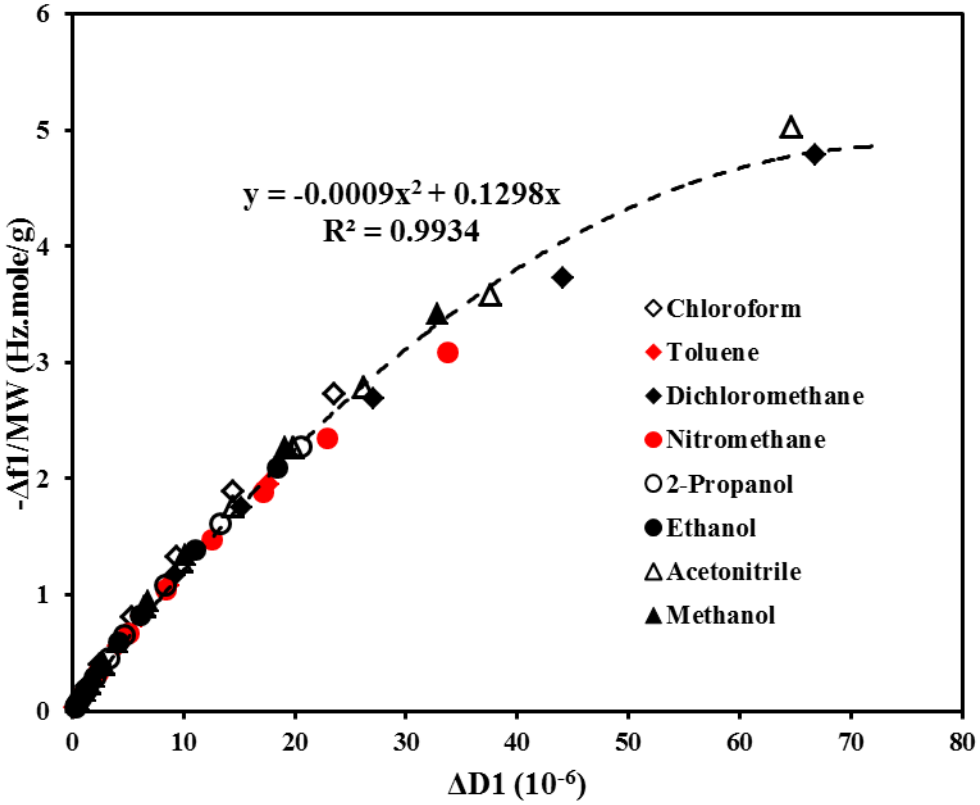

(b)

Fig. 7 (a) Frequency shift versus dissipation shift plots for the first harmonic of a QCM-D sensor coated with [HMPyr][PF_6]-PMMA during absorption of eight different organic vapors. Each analyte shows a second-degree polynomial curve with the coefficient of determination (R^2) nearly 1 (R^2 not shown in the graph). Concentration ranges of the vapors are 1.5 to 40% for methanol, 1 to 20% for acetonitrile, 1.5 to 40% for ethanol, 1 to 50% for 2-propanol, 1 to 15% for nitromethane, 1 to 15% for dichloromethane, 1 to 30% for toluene, and 1 to 15% for chloroform. Percentage refers to the percentage of saturated vapor concentration (b) Plot of the frequency shift-to-molecular weight ratio versus dissipation shift for the data from Figure 7a.

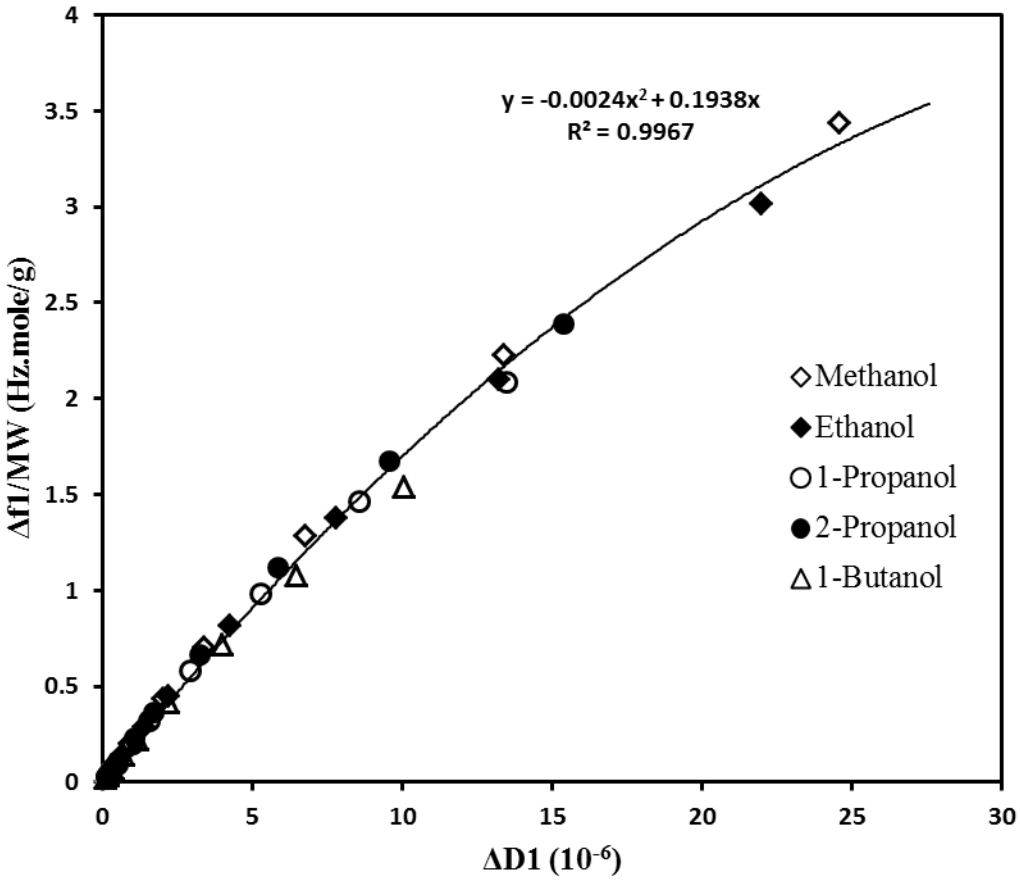

(a)

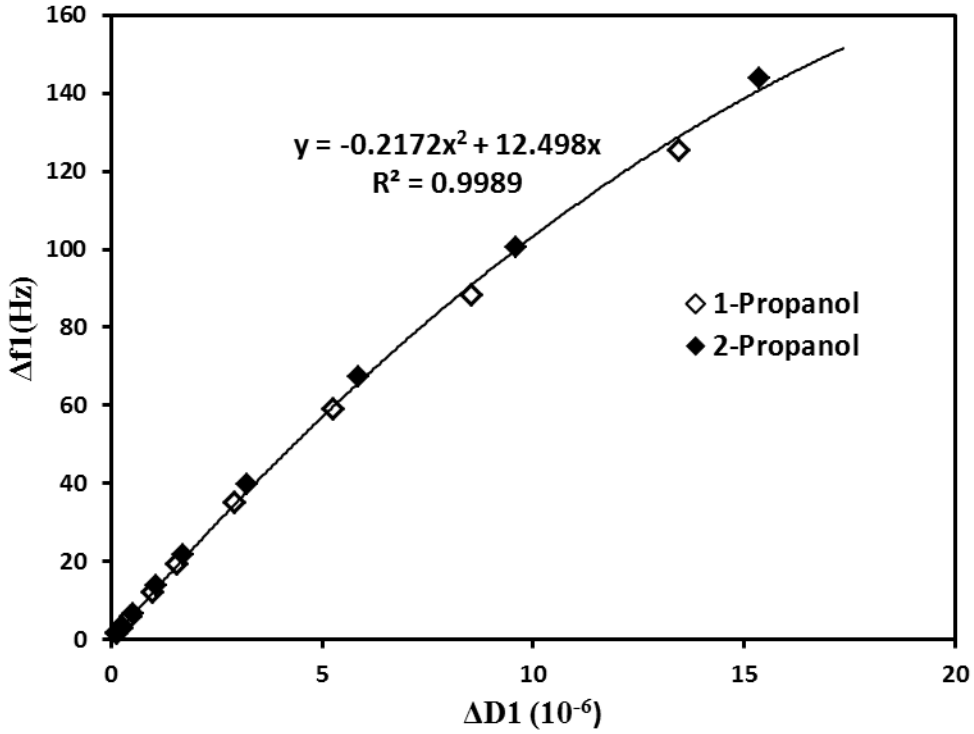

(b)

Fig. 8 (a) Frequency shift-to-molecular weight ratio versus dissipation shift plot for the first harmonic of a QCM-D sensor coated with [HMPyr][PF_6]-PMMA during absorption of five different alcohols. Concentration ranges of the vapors are 1.5 to 40% for methanol, 1 to 50% for all other alcohols and (b) plots of the frequency shift versus dissipation shift for n-propanol and isopropanol.

Given the fact that neither purely elastic nor purely viscous models could be used to explain our observations, we attempted to fit our data using viscoelastic models. This meant that all three parameters, t_f, η, and μ, were required for a fit to the model. The ranges of the fitting parameters were kept as follows: film viscosity between 0.0005 and 10 $kg.m^{-1}.s^{-1}$, film shear between 10 and $1x10^{10}$ Pa, and film thickness between $1x10^{-10}$ and $1x10^{-5}$ m (or corresponding mass between $1.3x10^{-7}$ and $1.3x10^{-2}$ $kg.m^{-2}$). Our data were then fit to both the Voigt and Maxwell viscoelastic models. Although we saw some improvements as compared to purely viscous or purely elastic models, the experimental Δf and ΔD values do not agree well with the fit values (see Fig. S17 and S18, ESI†). It must be stressed here that while fitting the data with the viscoelastic models, η and μ were assumed to be frequency independent. However, as pointed out by Reviakine, Johannsmann, and Richter,[23] this assumption cannot be justified for most of the viscoelastic materials. In fact, it has been recently demonstrated that the viscoelastic properties of ILs are frequency dependent.[38] In order to account for the frequency dependence of viscoelastic parameters, Q-Sense has introduced a new modeling option known as "extended viscoelastic model", which has been included in the QTools software. The frequency dependence of viscoelastic properties of the film was

assumed to follow a power law, and hence the relationships $\mu_n = \mu_0 \left(\frac{f_n}{f_o}\right)^{\alpha'}$ and $\eta_n = \eta_0 \left(\frac{f_n}{f_o}\right)^{\alpha}$ were used. The range chosen during modeling for α' was between 0 and 2 and for α between -2 and 0. Interestingly, we observed excellent agreement between the fit and experimental values of Δf and ΔD upon using the extended Maxwell viscoelastic model (Fig. 9a-c). Attempts to fit these data using the extended Voigt viscoelastic model (see Fig. S19a-c, ESI†) resulted in a several fold increase in χ^2. Hence, we conclude that the best model for describing the sensing response of our composite films is the extended Maxwell viscoelastic model. This inference is quite logical since the Maxwell viscoelastic model is more appropriate for liquids and amorphous solids,[29] and indeed the viscoelastic properties of ILs have previously been described using the Maxwell model.[39]

(a)

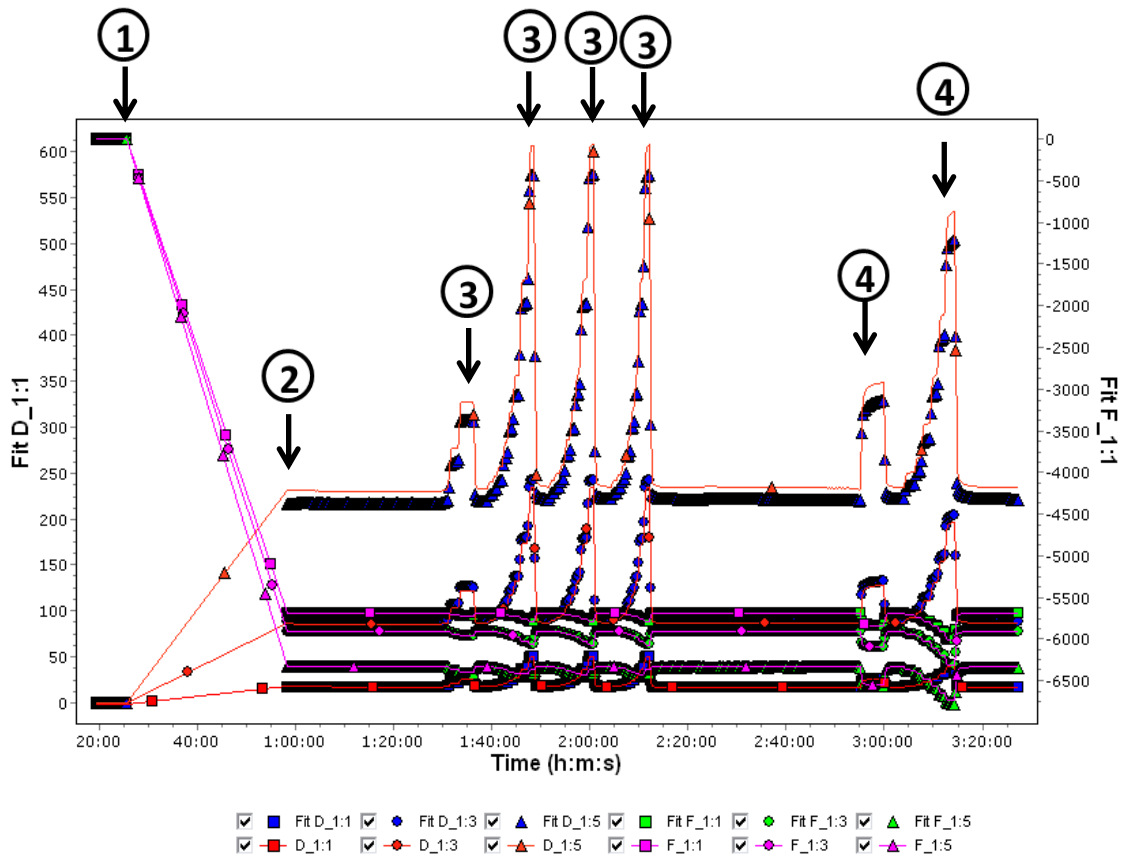

(b)

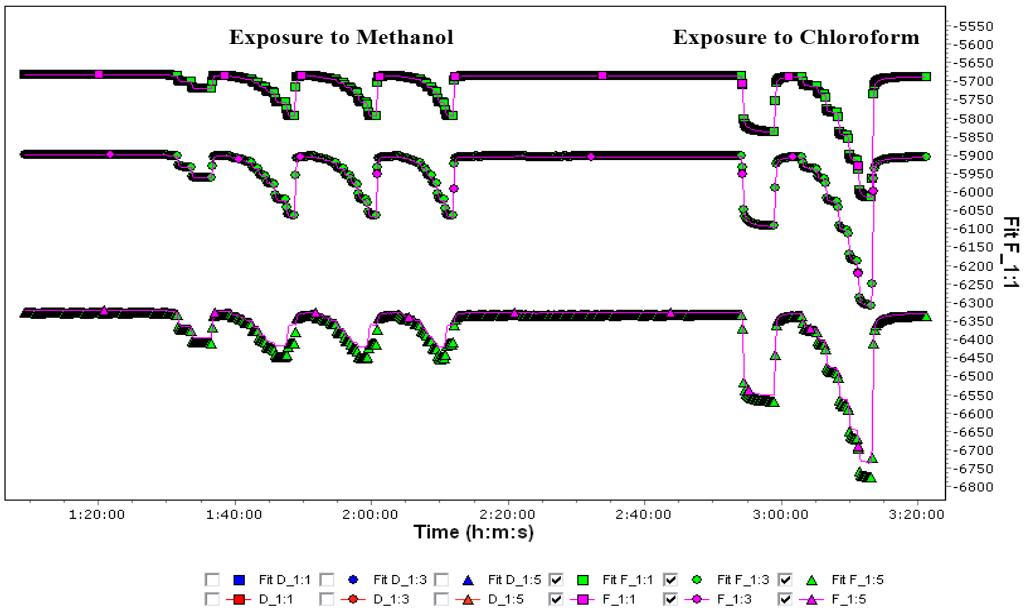

(c)

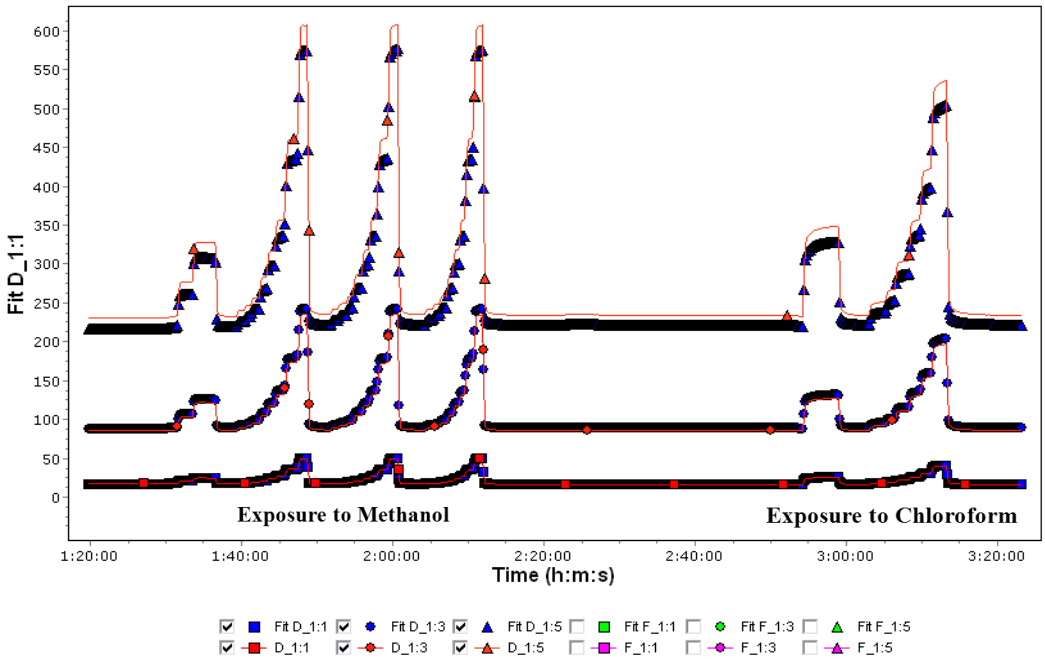

Fig. 9 (a) Representative QCM-D data displaying frequency and dissipation changes for the first, third, and fifth harmonics. Arrows represent: (1) bare quartz crystal, (2) after coating with [HMPyr][PF_6]-PMMA, (3) during exposure to methanol vapors, and (4) during exposure to chloroform vapors. The figure shows both the experimental and fit values of Δf and ΔD. The data were fit using extended Maxwell viscoelastic model. (b) Experimental and fit values of Δf and (c) experimental and fit values of ΔD during exposure to methanol and chloroform shown for clarity.

We should emphasize here that the viscoelastic models used above to analyze the QCM-D data assume a laterally homogeneous film. However, the films in our studies comprise isolated microdroplets of varying dimensions, and we are not aware of any model that can correctly describe the behavior of such laterally heterogeneous films. We note that it has been previously assumed such laterally heterogeneous films can be appropriately analyzed with models that have been used for laterally homogeneous films.[40-42] While this assumption has been shown to be questionable in liquids, the models based on laterally homogeneous films have been suggested to be applicable for laterally heterogeneous films in air.[23,43-45] Here, we simplify our analyses by assuming the film to be an "effective medium". However, it must be remembered that when analyzing heterogeneous films using models based on homogeneous films, the effective values of μ and η also depend on the heterogeneity of the film. Based on these discussions, we assert that our heterogeneous films are analogous to films of Maxwell viscoelastic fluids. For such films, Δf and ΔD are given by equations 5 and 6, respectively. However, these equations are for thin film where the thickness of the film (t_f) is much less than the viscous penetration depth (δ), $\delta = \sqrt{\frac{2\eta}{\rho_f \omega}}$, of the acoustic wave.[29,30,46] For thicker films, an increase or decrease in resonance frequency or dissipation can occur depending on the thickness and viscoelasticity.[30,46] ILs exhibit a wide variation in viscosities; for instance, at ambient pressure and 25 °C the viscosities of [HMIm][PF_6] and [HMIm][TFSI] are 607 and 68 mPa.s, respectively.[47] The densities of [HMIm][PF_6] and [HMIm][TFSI] at 25 °C are 1293 and 1372 kg.m^{-3} respectively.[47] For [HMIm][PF_6] at 25 °C, therefore, the penetration depth of the acoustic shear wave for the first (5MHz), third (15 MHz), and fifth (25 MHz) harmonics will be 5.47, 3.16, and 2.44 μm, respectively. Similarly, the penetration depth for [HMIm][TFSI] will be 1.78, 1.03, and 0.794 μm for the first, third, and fifth harmonics, respectively. The PF_6-based ILs are much more viscous than TFSI-based ILs, and pyridinium-based ILs are found to be more viscous than the equivalent imidazolium-based ILs.[48,49] It is observed that the modeled mass of the film before and during vapor absorption (or the mass of vapor absorbed) is very close to the Sauerbrey mass for the fundamental resonance frequency (Fig. S20, ESI†). However, substantial deviations can be seen at higher harmonics

(Fig. S20, ESI†). These observations are consistent with the studies reported by Vogt et al.[50] for hydrated polyelectrolyte films. It is further noted that both the elastic shear modulus and viscosity of the film decrease during vapor absorption (Fig. S21, ESI†); and similar behavior has been reported during addition of water to ILs.[38] The pure IL films could not be correctly modeled. However, a rough estimation is that the effective viscosity of the IL-PMMA may have increased up to six times as compared to that of the pure IL film. This ensures that the thickness of the composite film remains much lower than the decay length of the shear wave. Both PMMA and CA can increase the effective viscosity of the film. However, not all polymers were found to be equally effective; for example, polystyrene does not appear to modulate the viscoelastic properties of the IL films (data not shown).

After concluding that the sensing film behaves like a Maxwell viscoelastic fluid, we attempted to rationalize the relationship between molecular weight and $\frac{\Delta f}{\Delta D}$ ratio. For a Maxwell viscoelastic material, as shown in equation 5, Δf is the sum of two terms; the first term depends on mass, while the second term depends on the elastic modulus and density of the film. Hence, during analyte absorption, the first term varies as a function of mass absorbed independent of the analyte, whereas the second term, which comes as a small correction, may depend to some extent on the type of analyte absorbed. It is quite interesting to see that Δf is independent of the viscosity change so long as the film remains in the thin-film regime. It is also important to note that ΔD depends on viscosity, but is independent of elastic modulus. However, in the case of Voigt viscoelastic materials, both Δf and ΔD depend on the elasticity as well as viscosity of the film.[29,30] Upon rearranging equation 6, we obtain $\Delta D \approx \left(\frac{2\omega}{3\rho_q t_q}\right) \times \left(\frac{m_f^3}{\rho_f \eta}\right)$, where m_f is mass per unit area of the film. For a fixed harmonic, the first factor in this equation is constant, and hence ΔD depends on mass, viscosity, and density of the film. During vapor absorption, these three parameters i.e. m_f, ρ_f, and η undergo a change, and the total change in D is the sum of the contributions from the changes in all three parameters. For example, we have observed that deposition of 100.7 µg of composite film per cm^2 causes a dissipation factor change of 18.9 D (where $D=10^{-6}$) at the first harmonic. Absorption of 1.6 $\mu g.cm^{-2}$ of methanol by this film causes an increase in the dissipation factor to 51.9 D (change = 33.0 D). The increase in dissipation due to mass change, if viscosity and density were constant, would be only 0.89 D. Similarly, the change in dissipation due to density change would be much less than that contributed by mass change. Therefore, we conclude that the dissipation change is almost exclusively due to the viscosity change of the coating material.

We note that there have been extensive theoretical and experimental efforts to understand the viscosities of binary mixtures of ionic liquids and common molecular solvents; and many studies have demonstrated a dramatic decrease in the viscosity of an IL in the presence of molecular species.[51-61] One

of the most notable studies to predict viscosity of binary mixtures of IL and molecular solvent is that by Seddon and coworkers.[51] In that study, the authors systematically examined the influence of water and a number of organic solvents with different polarities on the viscosity of room temperature ionic liquids. Interestingly, the viscosity of the binary mixture was found to depend primarily on the mole fraction of the molecular component, irrespective of its polarity or dielectric constant. Hence, the authors proposed a single exponential equation to estimate the viscosity of such mixtures. This finding has been repeatedly confirmed in subsequent studies by many other research groups.[52,54,58] More rigorous rules have also been applied for more accurate predictions of the viscosities of mixtures.[58,61] For example, Wang et al.[58] examined the viscosity of a wide range of IL-molecular solvent systems by combining Eyring's absolute rate theory with activity coefficient models, and the results were compared with those obtained by use of Seddon's equation. The authors concluded that the Seddon equation always achieves satisfactory estimates of the viscosities of mixtures in IL-rich regions. Based on these discussions, we assert that the viscosity change of films in our study depends on the number of moles of vapor absorbed irrespective of their chemical characteristics. Such an assumption clearly explains the mole-dependent change in dissipation observed in our studies. Hence, simultaneous measurements of Δf and ΔD or ΔR of an IL or GUMBOS composite coated QCM sensor during vapor absorption provides a reasonable approximation of molecular weight of the vapor. Our findings should provide a sound foundation for further studies with respect to the discrimination of vapors based on molecular weights using these composite films.

Conclusions

The vapor-sensing application of a number of IL or GUMBOS-polymer composite films were studied with a QCM/QCM-D transducer. As many as 13 analytes were tested, and the data clearly demonstrate that an IL or GUMBOS-based QCM sensor offers an outstanding capability for estimating the molecular weight of organic vapor analytes. Viscoelastic modeling of the QCM-D data suggests that our composite films follow the Maxwell viscoelastic model. Based on this observation, a theoretical explanation for the observed relationship between the molecular weight of analytes and the QCM parameters is proposed. These types of materials when combined with QCM show considerable promise for discrimination of vapors based on their molecular weights. Further work is warranted to develop a sensor for more accurate prediction of molecular weights of vapors. Future work will focus on evaluation of viscosities of an extended range of IL-organic solvent mixtures and comparison of these data with the QCM observations. In addition, further understanding of the viscoelastic behavior of such films should be the focus of future studies.

Acknowledgements

This material is based upon work supported by the National Science Foundation under Grant number CHE-1243916. BPR acknowledges Archana Jaiswal, Biolin Scientific, for assistance in viscoelastic modeling.

Notes and references

1 W. Bourgeois, A. C. Romain, J. Nicolas and R. M. Stuetz, *J. Environ. Monit.*, 2003, **5**, 852.
2 A. P. F. Turner and N. Magan, *Nat. Rev. Microbiol.*, 2004, **2**, 161.
3 R. F. Machado, D. Laskowski, O. Deffenderfer, T. Burch, S. Zheng, P. J. Mazzone, T. Mekhail, C. Jennings, J. K. Stoller, J. Pyle, J. Duncan, R. A. Dweik and S. C. Erzurum, *Am. J. Respir. Crit. Care Med.,* 2005, **171**, 1286.
4 F. Roeck, N. Barsan and U. Weimar, *Chem. Rev.*, 2008, **108**, 705.
5 J. R. Carey, K. S. Susick, K. I. Hulkower, J. A. Imlay, K. R. C. Imlay, C. K. Ingison, J. B. Ponder, A. Sen and A. E. Wittrig, *J. Am. Chem. Soc.*, 2011, **133**, 7571.
6 K. Badjagbo, *WebmedCentral ENVIRONMENTAL MEDICINE*, 2012, **3**, WMC003174.
7 D. R. Walt, T. Dickinson, J. White, J. Kauer, S. Johnson, H. Engelhardt, J. Sutter and P. Jurs, *Biosens. Bioelectron.*, 1998, **13**, 697.
8 C. K. Ho, E. R. Lindgren, K. S. Rawlinson, L. K. McGrath and J. L. Wright, *Sensors*, 2003, **3**, 236.
9 K. S. Suslick, N. A. Rakow and A. Sen, *Tetrahedron*, 2004, **60**, 11133.
10 X. Jin, L. Yu, D. Garcia, R. X. Ren and X. Zeng, *Anal. Chem.*, 2006, **78**, 6980.
11 C. G. Jin, P. Kurzawski, A. Hierlemann and E. T. Zellers, *Anal. Chem.*, 2008, **80**, 227.
12 K. Scholten, F. I. Bohrer, E. Dattoli, W. Lu and E. T. Zellers, *Nanotechnology*, 2011, **22,** 125501.
13 E. Garcia-Berrios, T. Gao, J. C. Theriot, M. D. Woodka, B. S. Brunschwig and N. S. Lewis, *J. Phys. Chem. C*, 2011, **115**, 6208.
14 S. J. Park, O. S. Kwon, S. H. Lee, H. S. Song, T. H. Park and J. Jang, *Nano Lett.*, 2012, **12**, 5082.
15 Weiguo Huang, Jasmine Sinha, Ming-Ling Yeh, Josué F. Martínez Hardigree, Rachel LeCover, Kalpana Besar, Ana María Rule, Patrick N. Breysse, and H. E. Katz, *Adv. Funct. Mater.*, 2013, **23**, 4094.
16 N. J. Kybert, M. B. Lerner, J. S. Yodh, G. Preti and A. T. C. Johnson, *ACS Nano*, 2013, **7**, 2800.
17 Alona Bayn, Xinliang Feng and a. H. H. Klaus Müllen, *ACS Appl. Mater. Interfaces*, 2013, **5**, 3431.
18 C. D. Liang, C. Y. Yuan, R. J. Warmack, C. E. Barnes and S. Dai, *Anal. Chem.*, 2002, **74**, 2172.
19 A. Rehman and X. Zeng, *Acc. Chem. Res.*, 2012, **45**, 1667.
20 B. P. Regmi, J. Monk, B. El-Zahab, S. Das, F. R. Hung, D. J. Hayes and I. M. Warner, *J. Mater. Chem.*, 2012, **22**, 13732.
21 S. W. Lee and W. D. Hinsberg, *Anal. Chem.*, 2002, **74**, 125.
22 J. Schroder, R. Borngraber, F. Eichelbaum and P. Hauptmann, *Sens. Actuators, A*, 2002, **97-8**, 543.
23 I. Reviakine, D. Johannsmann and R. P. Richter, *Anal. Chem.*, 2011, **83**, 8838.
24 J. Schroder, R. Borngraber, R. Lucklum and P. Hauptmann, *Rev. Sci. Instrum.*, 2001, **72**, 2750.
25 M. Rodahl, F. Hook, A. Krozer, P. Brzezinski and B. Kasemo, *Rev. Sci. Instrum.*, 1995, **66**, 3924.
26 M. Rodahl and B. Kasemo, *Rev. Sci. Instrum.*, 1996, **67**, 3238.
27 D. Johannsmann, I. Reviakine and R. P. Richter, *Anal. Chem.*, 2009, **81**, 8167.
28 G. Sauerbrey, *Z. Phys.*, 1959, **155**, 206.
29 M. V. Voinova, Jonson M., and Kasemo B., *http://arxiv.org/abs/cond-mat/9906415*, 1999.
30 M. V. Voinova, M. Rodahl, M. Jonson and B. Kasemo, *Phys. Scr.*, 1999, **59**, 391.
31 J. G. Huddleston, A. E. Visser, W. M. Reichert, H. D. Willauer, G. A. Broker and R. D. Rogers, *Green Chem.*, 2001, **3**, 156.
32 J. Jacquemin, P. Husson, A. A. H. Padua and V. Majer, *Green Chem.*, 2006, **8**, 172.

33 A. S. Pensado, M. J. P. Comunas and J. Fernandez, *Tribol. Lett.*, 2008, **31**, 107.
34 J. C. Munro and C. W. Frank, *Macromolecules*, 2004, **37**, 925.
35 E. F. Irwin, J. E. Ho, S. R. Kane and K. E. Healy, *Langmuir*, 2005, **21**, 5529.
36 N. B. Eisele, F. I. Andersson, S. Frey and R. P. Richter, *Biomacromolecules*, 2012, **13**, 2322.
37 Because of the spatial heterogeneity of the film, the effective density of the film will be less than 1300 $kg.m^{-3}$. On rearranging equation 6, it can be seen product of viscosity and density in the denominator. As a consequecne, the modeled viscosity will be less than the effective viscosity, while other things remain unchaged. Strictly speaking, there is a very slight change in density during vapro absorption, but for simplicity the density is assumed to remain constant.
38 T. Yamaguchi, K. Mikawa and S. Koda, *Bull. Chem. Soc. Jpn.*, 2012, **85**, 701.
39 W. Makino, R. Kishikawa, M. Mizoshiri, S. Takeda and M. Yao, *J. Chem. Phys.*, 2008, **129,** 104510.
40 C. Larsson, M. Rodahl and F. Hook, *Anal. Chem.*, 2003, **75**, 5080.
41 I. Reviakine, F. F. Rossetti, A. N. Morozov and M. Textor, *J. Chem. Phys.*, 2005, **122**, 204711.
42 A. R. Patel and C. W. Frank, *Langmuir*, 2006, **22**, 7587.
43 E. Rojas, M. Gallego and I. Reviakine, *Anal. Chem.*, 2008, **80**, 8982.
44 D. Johannsmann, I. Reviakine, E. Rojas and M. Gallego, *Anal. Chem.*, 2008, **80**, 8891.
45 E. Tellechea, D. Johannsmann, N. F. Steinmetz, R. P. Richter and I. Reviakine, *Langmuir*, 2009, **25**, 5177.
46 G. McHale, R. Lucklum, M. I. Newton and J. A. Cowen, *J. Appl. Phys.*, 2000, **88**, 7304.
47 A. Muhammad, M. I. A. Mutalib, C. D. Wilfred, T. Murugesan and A. Shafeeq, *J. Chem. Thermodyn.*, 2008, **40**, 1433.
48 J. M. Crosthwaite, M. J. Muldoon, J. K. Dixon, J. L. Anderson and J. F. Brennecke, *J. Chem. Thermodyn.*, 2005, **37**, 559.
49 R. L. Gardas and J. A. P. Coutinho, *Fluid Phase Equilib.*, 2008, **266**, 195.
50 B. D. Vogt, E. K. Lin, W. L. Wu and C. C. White, *J. Phys. Chem. B*, 2004, **108**, 12685.
51 K. R. Seddon, A. Stark and M. J. Torres, *Pure Appl. Chem.*, 2000, **72**, 2275.
52 J. J. Wang, Y. Tian, Y. Zhao and K. Zhuo, *Green Chem.*, 2003, **5**, 618.
53 C. Comminges, R. Barhdadi, M. Laurent and M. Troupel, *J. Chem. Eng. Data*, 2006, **51**, 680.
54 M. T. Zafarani-Moattar and R. Majdan-Cegincara, *J. Chem. Eng. Data*, 2007, **52**, 2359.
55 W. Li, Z. Zhang, B. Han, S. Hu, Y. Xie and G. Yang, *J. Phys. Chem. B*, 2007, **111**, 6452.
56 I. B. Malham and M. Turmine, *J. Chem. Thermodyn.*, 2008, **40**, 718.
57 N. D. Khupse and A. Kumar, *J. Solution Chem.*, 2009, **38**, 589.
58 Y.G. Wang, D. X. Chen and X. K. OuYang, *J. Chem. Eng. Data*, 2010, **55**, 4878.
59 J. N. Canongia Lopes, M. F. C. Gomes, P. Husson, A. A. H. Padua, L. P. N. Rebelo, S. Sarraute and M. Tariq, *J. Phys. Chem. B*, 2011, **115**, 6088.
60 A. Jouyban, J. Soleymani, F. Jafari, M. Khoubnasabjafari and W. E. Acree, *J. Chem. Eng. Data*, 2013, **58**, 1523.
61 M. Tariq, T. Altamash, D. Salavera, A. Coronas, L. P. N. Rebelo and J. N. Canongia Lopes, *ChemPhysChem*, 2013, **14**, 1956.